Investigation of the spectroscopic properties of Nd^{3+}-doped phosphate glasses

2000 J. Phys.: Condens. Matter 12 3181

(http://iopscience.iop.org/0953-8984/12/13/324)

J. Phys.: Condens. Matter **12** (2000) 3181–3193. Printed in the UK PII: S0953-8984(00)04512-4

Investigation of the spectroscopic properties of Nd^{3+}-doped phosphate glasses

M Ajroud†, M Haouari†, H Ben Ouada†, H Maaref†, A Brenier‡ and C Garapon‡

† Département de Physique, Faculté des Sciences de Monastir, 5000 Monastir, Tunisia
‡ Laboratoire de Physico-Chimie des Matériaux Luminescents, UMR 5620 CNRS, Université Lyon 1, France

Received 24 May 1999, in final form 20 December 1999

Abstract. Optical properties of Nd^{3+}-doped phosphate glasses have been studied on the basis of the Judd–Ofelt theory. With the intermediate cross-section value and the weak Ω_4/Ω_6 parameter, we expect a relatively prominent $^4F_{3/2} \rightarrow {}^4I_{11/2}$ laser emission.

The quenching effect of the emission intensity is discussed in terms of cross-relaxation between the Nd^{3+} ions as well as energy transfer processes within the host matrix. From the investigation of the decay rate from the $^4F_{3/2}$ state with the neodymium concentration, we suggest that self-quenching is insured by dipole–dipole interaction. This result was also confirmed by the simulation of the decay with the Inokuti–Hyrayama model.

1. Introduction

Recent decades have witnessed a growing interest in the investigation of spectroscopic properties of rare-earth-doped glasses. This interest arises from the need of these materials for lasers and optical fibres [1, 2], acousto-optic modulators [3] and planar waveguides [4].

Because of their thermo-optical quality, phosphate glasses have proved to be excellent host materials for solid-state lasers. Furthermore, they are easy to prepare in various compositions and they preserve the useful properties upon the introduction of a significant amount of active ions [2–5].

Among the trivalent rare earth ions, Nd^{3+} is one of the most interesting ones due to its several absorption bands within the pump excitation domain and the possibility of lasing at different wavelengths at room temperature [3].

In the present work, a spectroscopic study of Nd^{3+}-doped phosphate glasses is reported. By the use of Judd–Ofelt theory, we were able to determine their optical properties and to characterize the particular laser transition $^4F_{3/2} \rightarrow {}^4I_{11/2}$ by investigating its quantum efficiency as well as the non-radiative relaxation affecting emission.

2. Theory

The spectroscopic properties of trivalent rare earth ions in solid media and solution are usually investigated by means of the Judd–Ofelt (J–O) model [6, 7]. According to this model, these properties are characterized by three phenomenological parameters Ω_2, Ω_4 and Ω_6 which

0953-8984/00/133181+13$30.00

depend on the local environment and can be determined experimentally from the measurements of absorption spectra and the refractive index of the host material.

In the J–O treatment, the oscillator strength of an electronic transition of average frequency ν from a level J to another level J' is the most host-dependent quantity and is given by

$$f(aJ, bJ') = \frac{8\pi^2 m\nu}{3(2J+1)he^2n^2}[\chi_{ED}S_{ED}(aJ, bJ') + \chi_{MD}S_{MD}(aJ, bJ')] \quad (1)$$

where e and m are the charge and the mass of the electron respectively and h is Planck's constant. The factors χ_{ED} and χ_{MD} are local field corrections and are functions of the medium refractive index n: $\chi_{ED} = n(n^2+2)^2/9$ and $\chi_{MD} = n^3$. S_{ED} and S_{MD} are the electric dipole and magnetic dipole line strengths respectively and are given by the following equations:

$$S_{ED}(aJ, bJ') = e^2 \sum_{t=2,4,6} \Omega_t |\langle 4f^N aJ||U^{(t)}||4f^N bJ'\rangle|^2 \quad (2)$$

$$S_{MD}(aJ, bJ') = \frac{e^2\hbar^2}{4m^2c^2}|\langle 4f^N aJ||\vec{L} + 2\vec{S}||4f^N bJ'\rangle|^2 \quad (3)$$

where the terms $\langle \ldots||U^{(t)}||\ldots\rangle$ are the doubly reduced matrix elements of the unit tensor operators calculated in the intermediate-coupling approximation and which are host independent but constant characteristics to each transition. The $\langle \ldots||\vec{L} + 2\vec{S}||\ldots\rangle$ terms are the magnetic dipole operator matrix elements. However, the contribution of electric dipole transitions in the oscillator strengths is usually the most important.

The coefficients Ω_2, Ω_4 and Ω_6 are the intensity parameters, which contain the effects of the crystal-field terms, radial integrals of electrons and so on. They are determined by a least-squares fit of the theoretical oscillator strengths (1) to the values of measured oscillator strengths calculated from optical absorption spectrum using the equation [8]

$$f_{exp} = \frac{mc^2}{\pi e^2 Nd}\int D_0(\nu)\,\mathrm{d}\nu \quad (4)$$

where c is the vacuum light velocity, N is the Nd^{3+} concentration (in cm^{-3}), d is the sample thickness and $\int D_0(\nu)\,\mathrm{d}\nu$ is the integrated optical density determined numerically. In order to evaluate the validity of the intensity parameters obtained by the fitting, the deviation parameter value (δ_{ms}) was calculated by the relation

$$\delta_{ms} = \frac{\sum(f_c - f_m)^2}{N_{param} - N_{trans}} \quad (5)$$

where f_c and f_m are the calculated and the measured line strengths, respectively, and summation is taken over all the bands used to calculate the $\Omega_{(t)}$ parameters. By means of these parameters, one can estimate the spontaneous emission probabilities through the equation:

$$A(aJ, bJ') = \frac{64\pi^4\nu^3}{3h(2J+1)c^3}[\chi_{ED}S_{ED}(aJ, bJ') + \chi_{MD}S_{MD}(aJ, bJ')]. \quad (6)$$

Also, one defines the radiative lifetime, τ_r, for a given state J and the branching ratio for an $aJ \to b''J''$ transition from the same J level by the following equations:

$$\tau_r(J) = \left(\sum_{J'} A(aJ, bJ')\right)^{-1} \quad (7)$$

$$\beta_{JJ''} = A(aJ, b''J'')\left(\sum_{J'} A(aJ, bJ')\right)^{-1}. \quad (8)$$

Here, the summation is over all transitions from the excited state to terminal levels.

For direct excitation, the luminescence quantum yield, η, is defined as

$$\eta = \frac{\text{emitted light intensity}}{\text{absorbed pump intensity}} = \frac{\tau_m}{\tau_r} \tag{9}$$

where τ_m is observed lifetime determined from the luminescence decay.

For an $aJ \rightarrow bJ'$ spontaneous transition having the probability $A(aJ, bJ')$, the stimulated emission cross-section is given by the formula

$$\sigma(aJ, bJ') = \frac{\lambda_p^4}{8\pi cn^2 \Delta\lambda_{eff}} A(aJ, bJ'). \tag{10}$$

Here, n is the host refractive index and λ_p is the emission line wavelength which has an effective band width of $\Delta\lambda_{eff}$ determined by the relation

$$\Delta\lambda_{eff} = \frac{1}{I_{max}} \int I(\lambda)\, \mathrm{d}\lambda. \tag{11}$$

3. Sample preparation

Neodymium-doped phosphate glasses were prepared by melting reagents in a platinum crucible, in an electric furnace heated to 1350 °C in an air atmosphere. The melt was then poured onto a stainless plate and annealed at 400 °C. Finally, the samples were polished to obtain slides for optical measurements. The glasses were prepared in the following composition: 28.5 mol% of BaO, 14.5 mol% of K_2O and 57 mol% of P_2O_5.

This composition was selected because it allows us to dissolve a significant amount of neodymium oxide without precipitation. Glasses were doped by adding x wt% of Nd_2O_3 to the starting composition.

4. Results

4.1. Optical absorption

The optical absorption spectrum of the diluted sample ($N_{Nd} = 1.083 \times 10^{20}$ cm^{-3}) consists of a large number of lines (figure 1) attributed to transitions occurring within the 4f shell of the Nd^{3+} ion.

We report in table 1 the experimental oscillator strengths estimated from this spectrum and the calculated ones using the unit tensor matrix elements determined by Judd [6]. The

Table 1. Transition frequencies, calculated and measured oscillator strengths (OSs).

Excited level $(S'L')J'$	Position (nm)	Frequency (cm^{-1})	Measured OS (10^{-6})	Calculated OS (10^{-6})
$^4F_{3/2}$	872	11 468	1.82	1.94
$^4F_{5/2}$, $^2H_{9/2}$	801	12 484	6.76	8.85
$^4F_{7/2}$, $^4S_{3/2}$	746	13 404	6.63	4.79
$^4F_{9/2}$	684	14 620	0.75	1.30
$^4G_{5/2}$, $^2G_{7/2}$	582	17 182	15.68	15.59
$^4G_{7/2}$, $^4G_{9/2}$, $^2K_{13/2}$	524	19 083	4.30	4.05
$^4G_{11/2}$, $^2G_{9/2}$ $^4G_{3/2}$, $^2K_{15/2}$	476	21 008	4.57	1.73
$^4P_{1/2}$, $^2D_{5/2}$	428	23 364	2.00	3.09
$^2D_{3/2}$, $^2D_{5/2}$, $^4I_{11/2}$, $^2D_{1/2}$, $^4L_{15/2}$	355	28 169	10.02	2.48

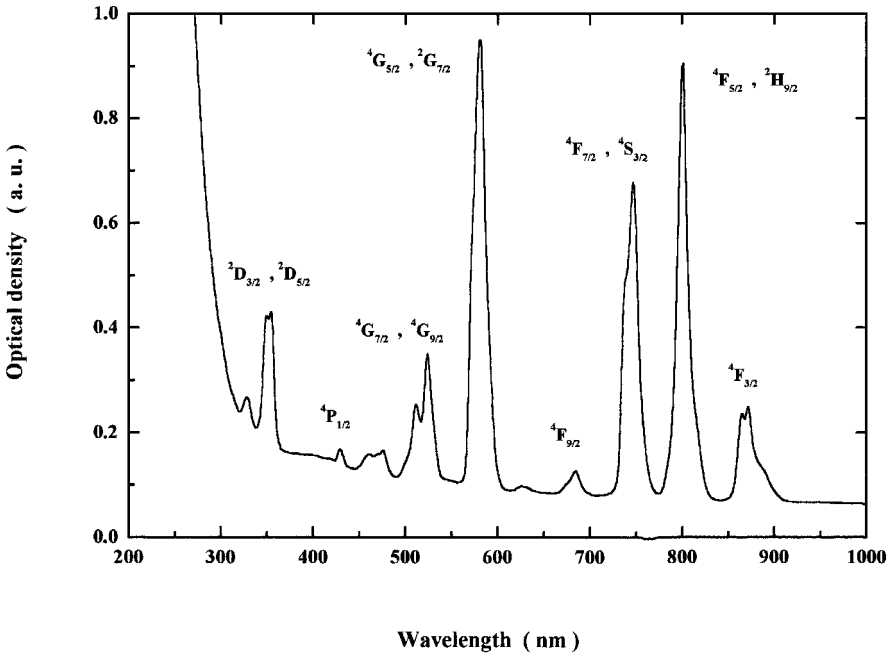

Figure 1. Absorption spectrum of the neodymium-doped glass system ($N_{Nd} = 1.083 \times 10^{20}$ cm^{-3}).

deviation parameter $\delta_{mc} = 2.2 \times 10^{-6}$ is of the same order in magnitude as those generally found for rare earth ions in glasses.

4.2. Emission

The emission spectra of the neodymium-doped phosphate glasses consist of three large and non-symmetric bands centred nearly at 896, 1059 and 1324 nm (figure 2) which are attributed respectively to the $^4F_{3/2} \rightarrow {}^4I_{9/2}$, $^4I_{11/2}$ and $^4I_{13/2}$ transitions. The emission probabilities and the branching ratios corresponding to these transitions from the $^4F_{3/2}$ state are calculated using the intensity parameters $\Omega_{(t)}$ and are given in table 2. The probability values have allowed us to determine the radiative lifetime of the $^4F_{3/2}$ state.

Table 2. Transition probabilities and branching ratios of the emission lines.

$(S'L')J'$	λ_m (nm)	$\langle {}^4F_{3/2} \|\| U^{(4)} \|\| (S'L')J' \rangle$	$\langle {}^4F_{3/2} \|\| U^{(6)} \|\| (S'L')J' \rangle$	A (s^{-1})	β
$^4I_{9/2}$	896	0.230	0.056	849	0.35
$^4I_{11/2}$	1059	0.142	0.407	1232	0.53
$^4I_{13/2}$	1324	0.000	0.212	242	0.11

The $^4F_{3/2} \rightarrow {}^4I_{11/2}$ transition band is the most intense and has an effective width of 29.3 nm. Following its intensity evolution with the Nd^{3+} concentration (figure 3), we observe a noticeable decrease for concentrations higher than 4.3×10^{20} cm^{-3}. Furthermore, the luminescence decay of this transition was examined for different neodymium concentrations. Only those relative to low concentrations ($N < 4.3 \times 10^{23}$ cm^{-3}) could be described by an exponential function (figure 4). The luminescence mean lifetimes are consequently estimated

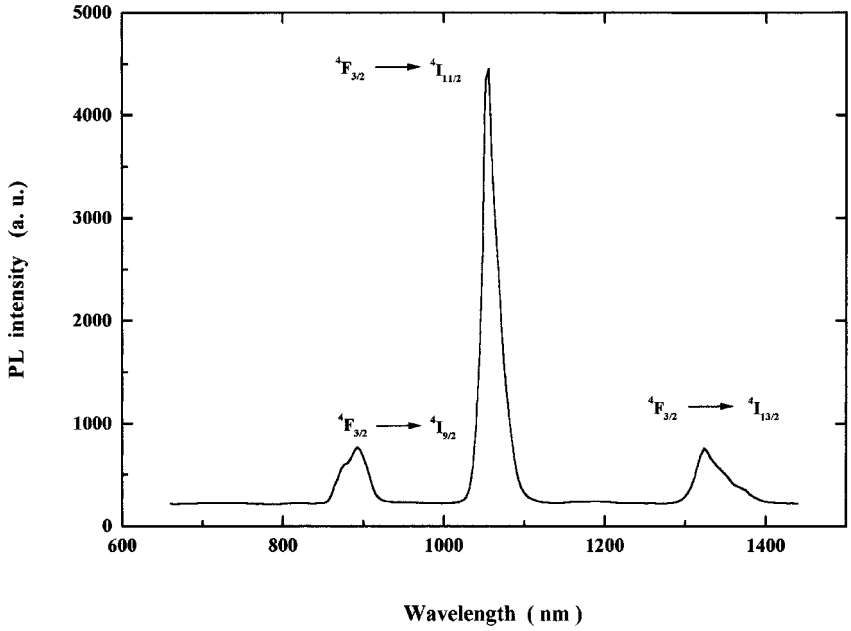

Figure 2. Neodymium emission spectrum at room temperature.

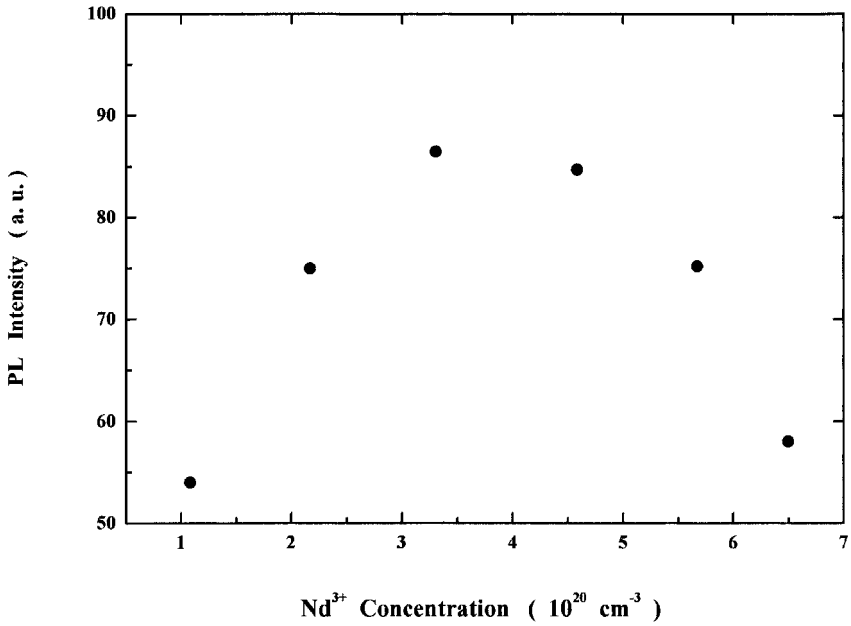

Figure 3. The $^4F_{3/2} \rightarrow {}^4I_{11/2}$ line intensity evolution as a function of the Nd^{3+} ion concentration.

using the relation [9]:

$$\bar{\tau} = \frac{1}{I_0} \int I(t)\,\mathrm{d}t \tag{12}$$

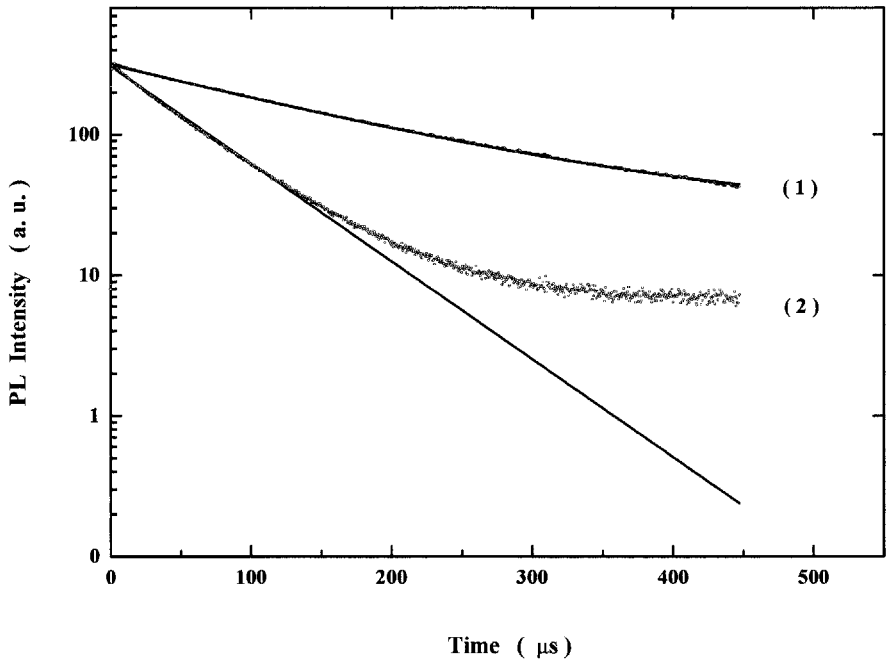

Figure 4. Luminescence decay of the Nd^{3+} $^4F_{3/2}$ state. (○): experimental, (——): theoretical, (1): $N_{Nd} = 1.083 \times 10^{20}$ cm^{-3}, (2): $N_{Nd} = 5.413 \times 10^{20}$ cm^{-3}.

where I_0 is the luminescence intensity at $t = 0$. The stimulated emission cross-section of the $^4F_{3/2} \rightarrow {}^4I_{11/2}$ transition was calculated by the relation [10]:

$$\sigma = \frac{2\pi^3 e^2}{27c} \frac{\lambda_p}{\Delta\lambda_{eff}} \frac{(n^2+2)^2}{n} (\Omega_4 [U^{(4)}]^2 + \Omega_6 [U^{(6)}]^2) \tag{13}$$

where $[U^{(4)}]^2 = 0.1423$ and $[U^{(6)}]^2 = 0.4070$. With the Ω_4 and Ω_6 intensity parameters found in this study, we obtain a σ value of 2.78×10^{-20} cm^{-2}.

5. Discussion

5.1. Absorption and emission spectrum analysis

According to Jørgensen and Reisfeld [11], the Ω_2 parameter is a measure of the covalence degree related to the established rare earth ion—ligand bonds whereas the Ω_6 is relative to the stiffness of the host matrix. Moreover, the Ω_2 parameter reflects the non-symmetry of the Nd^{3+} local environment; the weaker the Ω_2 value, the more centrosymmetrical the ion site is and the more ionic its chemical bonds with the ligands are.

The high value of the maximum splitting of the $^4I_{9/2}$ Nd^{3+} ground state by the crystal field ($\Delta E = 649$ cm^{-1}), estimated from the study of the $^4I_{9/2} \rightarrow {}^2P_{1/2}$ absorption transition in this vitreous system (figure 1) is higher than that reported by Auzel [12], which indicates obviously that the concentration quenching phenomenon is possible in this system.

The transitions having intensity dominated by the Ω_2 parameter are known as hypersensitive and obey the following selection rules:

$$\Delta J \leqslant 2 \qquad \Delta L \leqslant 2 \qquad \Delta S = 0.$$

Table 3. Judd–Ofelt parameters of the Nd^{3+} ion in different vitreous systems [17].

Vitreous system	Ω_2 (10^{-20} cm^2)	Ω_4 (10^{-20} cm^2)	Ω_6 (10^{-20} cm^2)	Ω_4/Ω_6
Silicates	3.2	4.6	4.8	0.95
Phosphates	3.3	5.0	5.6	0.89
Borates	4.3	3.6	4.7	0.76
Fluoroberyllates	0.2	3.9	4.6	0.85
Fluorophosphates	1.8	4.1	5.0	0.82
Our system	3.28	3.54	4.67	0.76

Table 4. Variation domain of the $^4F_{3/2} \rightarrow {}^4I_{11/2}$ transition spectroscopic properties in different vitreous systems [17].

Vitreous system	n	σ (10^{-20} cm^2)	λ (nm)	$\Delta\lambda$ (nm)	τ (μs)
Silicates	1.46–1.75	0.9–3.6	1057–1065	34–43	170–1090
Phosphates	1.49–1.63	2.0–4.8	1052–1057	22–35	280–530
Tellurites	2.0–2.1	3.0–5.1	1056–1053	26–31	140–240
Fluorophosphates	1.41–1.56	2.2–4.3	1050–1056	27–34	310–570
Fluoroberyllates	1.28–1.38	1.6–4.0	1046–1050	19–28	460–1030
Our system	1.51	2.78	1059	29.3	430

The Nd^{3+} absorption line centred at nearly 580 nm and corresponding to the $^4I_{9/2} \rightarrow {}^4G_{5/2}$ transition is the most intense. This result is expected since that this transition obeys the latter rules and has consequently its intensity dominated by the Ω_2 parameter contribution which changes significantly with the ion local environment and to which corresponds the highest value of the unit tensor matrix element $[U^{(2)}]$.

According to Jacobs and Weber [13], the neodymium emission intensity could be characterized uniquely by the Ω_4 and Ω_6 parameters. Thus, we utilize the so-called spectroscopic quality parameter, equal to the ratio (Ω_4/Ω_6). The smaller this parameter value, the more intense the laser transition $^4F_{3/2} \rightarrow {}^4I_{11/2}$ is. The obtained value of this parameter in our glass system, 0.76, indicates that this transition has relatively an important intensity compared to other vitreous systems (table 3).

The emission peak position is related to the covalence degree of the Nd^{3+}–ligand bonds in the matrix. The more covalent these bonds, the weaker the electron–electron interaction in the 4f shell and the lower the transition energy is [14]. Based on the above mentioned arguments, the obtained value of the $^4F_{3/2} \rightarrow {}^4I_{11/2}$ emission peak wavelength (1059 nm) suggests that in this matrix, the Nd^{3+} ion interacts strongly with its ligands compared to other systems (table 4) [14, 15].

Despite the presence of several intense bands in the higher energy region, those situated at nearly 746 and 801 nm are the most interesting because of their non-radiative coupling to the $^4F_{3/2}$ level from which the Nd^{3+} ion relaxes radiatively to the $^4I_{9/2}$, $^4I_{11/2}$ and $^4I_{13/2}$ states. The radiative decay of the $^4F_{3/2}$ state is slow (190 μs) due to the interdiction of electric dipole transitions by the selection rules: $\Delta J = 0, \pm 1$ and to the relatively important energy gap between this level and the next lower one [16].

5.2. Emission cross-section

Having estimated the $^4F_{3/2} \rightarrow {}^4I_{11/2}$ emission cross-section in our system, we can conclude that the σ value is much higher than those obtained in other systems (table 4). We can attribute

this fact to the introduction of the K^+ modifier ion having the effect of reducing the emission bandwidth [17]. Furthermore, our glass composition, having the advantage of containing large phosphate proportions, allows the increase of the absorption and the stimulated emission cross-section according to Seeber *et al* [18]. This result is also explained in the light of other important structural considerations. Indeed the high phosphate content allows the rare earth to establish a more symmetric and chemically uniform coordinate sphere which leads to a narrower linewidth and a negligible inhomogeneous broadening [19].

5.3. Luminescence decay and non-radiative processes

The radiative lifetime of the $^4F_{3/2}$ state depends upon the values of Ω_4 and Ω_6 parameters as well as the host refractive index. It represents a mean value over the different sites occupied by the Nd^{3+} ions and it is higher than that determined experimentally from the luminescence decay. To explain this reduction, we shall consider all the processes contributing to the Nd^{3+} relaxation. With weak concentrations ($N < 4.3 \times 10^{20}$ cm^{-3}), the non-radiative relaxations due to the ion–ion interactions are negligible and the radiative lifetime is often in agreement with that measured experimentally. Nevertheless, the lifetimes obtained in our study could not be attributed uniquely to radiative relaxations but also to the non-radiative ones being more probable and effective in phosphate glasses, due to their relatively important vibrational frequencies, than in other oxide or fluoride glasses.

The emitting state lifetime measured from the luminescence temporal evolution takes into account, consequently, the contribution of all processes and it is generally lower than the radiative lifetime τ_r. The total decay rate, being the inverse of τ, is then denoted as

$$\frac{1}{\tau} = A_r + W_{n-r}. \tag{14}$$

Here, A_r and W_{n-r} represent respectively the radiative and the non-radiative decay rates.

In phosphate glasses, there are principally four non-radiative processes (figure 5) contributing to the reduction of the Nd^{3+} $^4F_{3/2}$ excited state [18, 20]: multiphonon relaxation, concentration quenching, energy transfer to another doping impurity such as transition metal ions or other rare earth ions and energy transfer to hydroxyl groups OH^-. In general, the non-radiative decay rate is expressed by

$$W_{n-r} = W_{m-p} + W_{c-q} + W_{e-t} + W_{OH} \tag{15}$$

where W_{m-p}, W_{c-q}, W_{e-t} and W_{OH} are the non-radiative decays corresponding respectively to the multiphonon process, concentration quenching and to the energy transfer processes to another ion or to the hydroxyl groups OH^-.

5.3.1. Multiphonon processes. This phenomenon, resulting from the local crystal field modulation by the ligand vibrations, causes an energy level broadening and a spread of the electron transition frequencies over a relatively important domain. The temperature dependence of the $^4F_{3/2}$ state lifetime (figure 6) exhibits a relatively important thermal extinction of the Nd^{3+} luminescence between 9 and 100 K. This extinction could be attributed to non-radiative relaxations by phonon emission and results in both the lifetime and the luminescence quantum yield reduction.

Owing to the high vibration frequencies of the phosphate groups (1120 cm^{-1}) [21], this process is more probable in phosphate glasses than in the other oxide (exempting the borate glasses) or the halide vitreous systems. However, the experience showed that the multiphonon process contribution to the decay does not exceed 10% in phosphate glasses at room temperature. According to Miyakawa and Dexter [22], this is due to the relatively

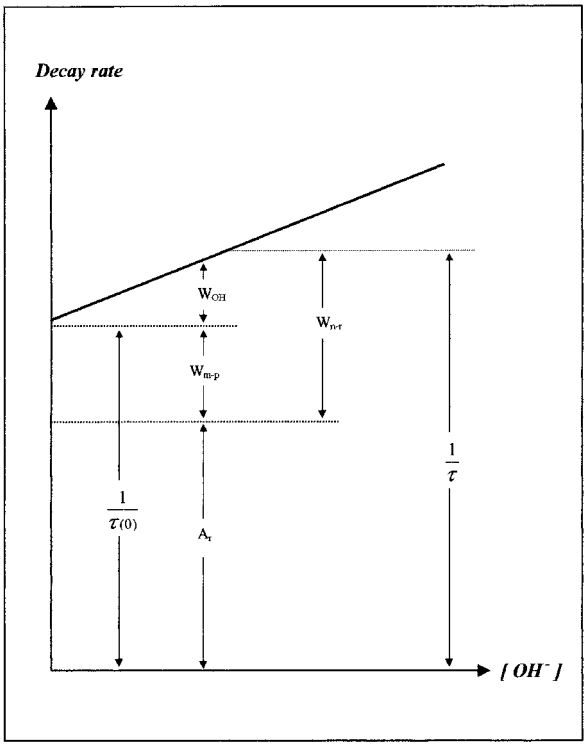

Figure 5. The different processes contributing to the Nd^{3+} ion luminescence decay (after [20]).

large energy gap between the $^4F_{3/2}$ state and the next lower J manifold (7407 cm^{-1}). Other authors [23, 24] have attributed the luminescence thermal extinction to a phonon assisted energy transfer between Nd^{3+} ions. This transfer process between two identical ions is well understood taking account of the transition energy weak spread from the $^4F_{3/2}$ state to the J states due to the structural disorder of the other glasses.

5.3.2. Energy transfer to the OH^- groups. The relaxation rate W_{OH}, usually weak in other oxide glasses, could be important in phosphate glasses especially if the OH^- group concentration is high enough. These hydroxyl groups of the water molecules existing initially in the vitreous matrix and having relatively high vibration frequencies compared to those of ligands (3000 cm^{-1}) contribute considerably to the non-radiative deexcitation of Nd^{3+} ions and could cause a luminescence quenching in phosphate glasses even at low temperature (figure 6). Seeber *et al* [18] have yet observed a considerable reduction of the $^4F_{3/2}$ state lifetime following the increase of the phosphate content in the glass composition. Moreover, studies of the neodymium-doped phosphate glasses have showed that the probability of luminescence quenching by the OH^- groups increases with the radius of the modifier cation [25]. In general, and to have an efficient laser yield in Nd^{3+}-doped phosphate glasses, the OH^- group concentration should not exceed 100 ppm [1] which has to be realized by a judicious control of the melting conditions [25].

5.3.3. Concentration quenching. This process appears when the Nd^{3+} concentration becomes important. The ions can interact efficiently resulting in an energy transfer from an excited ion to

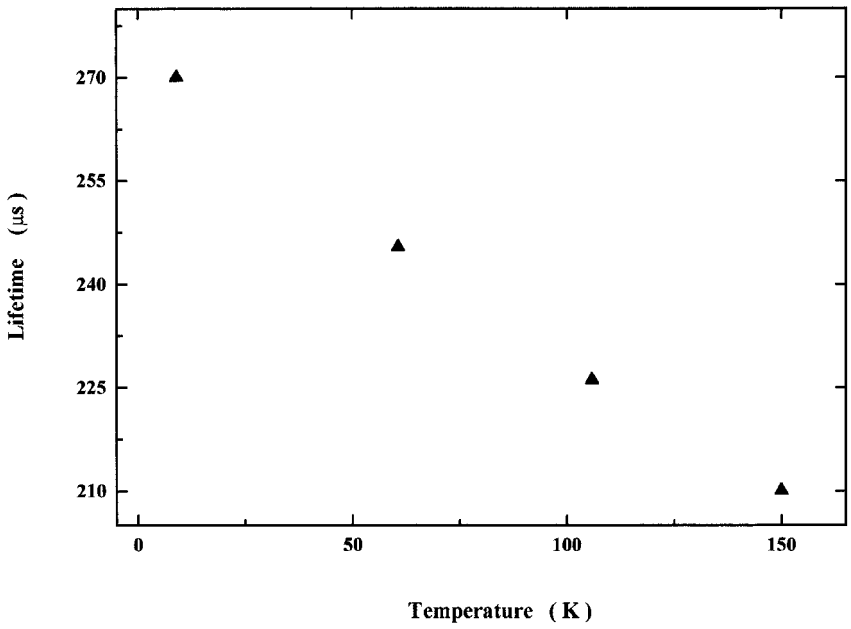

Figure 6. Temperature dependence of the $^4F_{3/2}$ state lifetime ($N_{Nd} = 2.166 \times 10^{20}$ cm^{-3}).

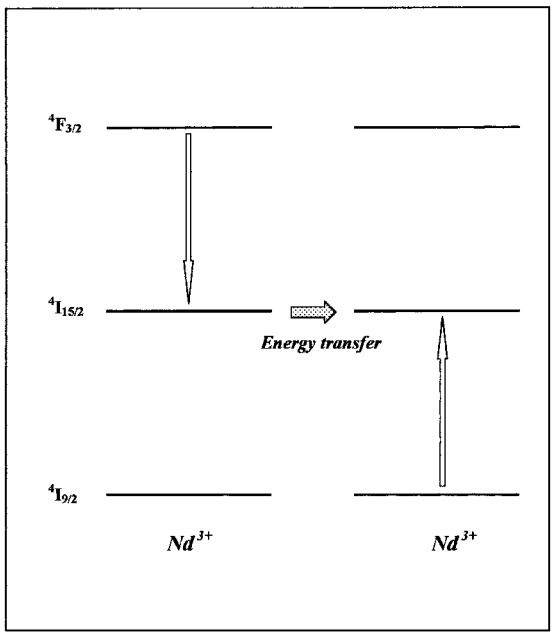

Figure 7. Luminescence extinction by an energy transfer process within the Nd^{3+}–Nd^{3+} pair.

another one initially in its ground state. The two ions pass then to an intermediate excited state from which they relax non-radiatively. If the concentration is sufficiently high, luminescence extinction can occur. The luminescence decays observed for the relatively high concentration

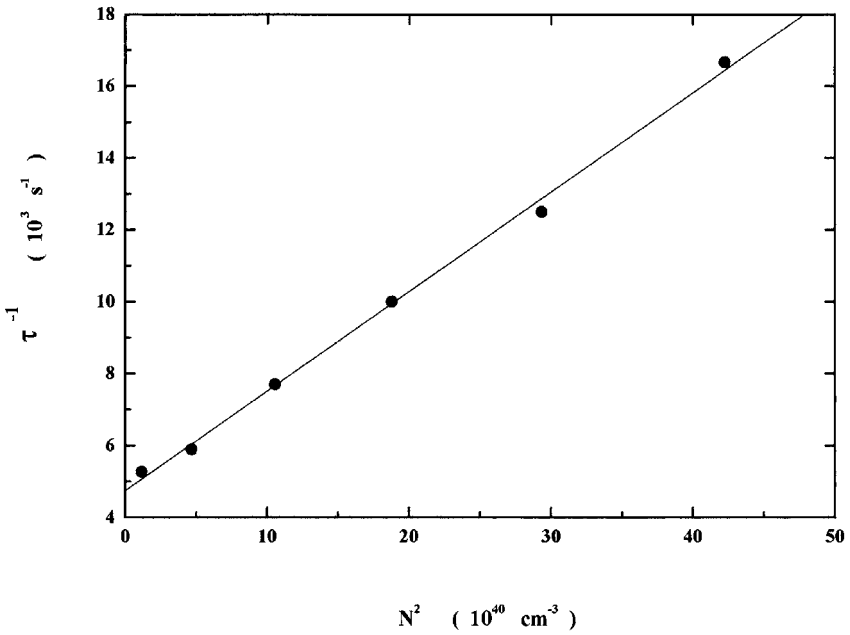

Figure 8. Non-radiative relaxation rate variation as a function of the squared neodymium concentration.

could not be described by a simple exponential and the higher the concentration, the more rapid they are. This result could be explained by the presence of an excitation energy transfer from an Nd^{3+} ion being in the excited $^4F_{3/2}$ state to another one initially in its ground state; then the two ions relax non-radiatively to their $^4I_{9/2}$ ground state (figure 7). This transfer can occur either by an exchange coupling or by electric multipolar interactions. The exchange interactions result from an important overlap between the donor and the acceptor electron clouds; thus, they depend upon the spatial spread of the wave functions as well as the mean distance between the two ions. The reach of the 4f electron wave functions does not exceed 0.3 Å and it is less than the mean distance between the ions (a few Å). Within the concentration range utilized in this study, we can neglect the exchange coupling effect and consider only the multipolar interactions.

Figure 8 shows that the non-radiative relaxation rate varies linearly with the squared concentration, indicating thus that the energy transfer in the Nd^{3+}–Nd^{3+} pair is insured by a dipole–dipole interaction. In fact, according to Dexter [26], the energy transfer rate occurring by an electric dipole interaction is proportional to the inverse of the sixth power of the distance separating the two ions and consequently to the squared concentration.

In addition, and due to the selection rules $\Delta J = 0, \pm 1$, only the dipole–dipole interactions are allowed. As a consequence, we have obtained a good simulation of the luminescence decay curves for the higher concentrations ($N > 4.3 \times 10^{20}$ cm^{-3}) (figure 9) by the theoretical expression for dipole–dipole type interaction [27]

$$\Phi(t) = \Phi_0 \exp\left[-\frac{t}{\tau} - \frac{4}{3}\pi\Gamma\left(1 - \frac{3}{s}\right) N R_0^3 \left(\frac{t}{\tau}\right)^{3/S} \right] \tag{16}$$

where $\Gamma(x)$ is the Euler function, s is a number which equals 6 and R_0 is a critical radius corresponding to the equality between the non-radiative intrinsic Nd^{3+} relaxation and the

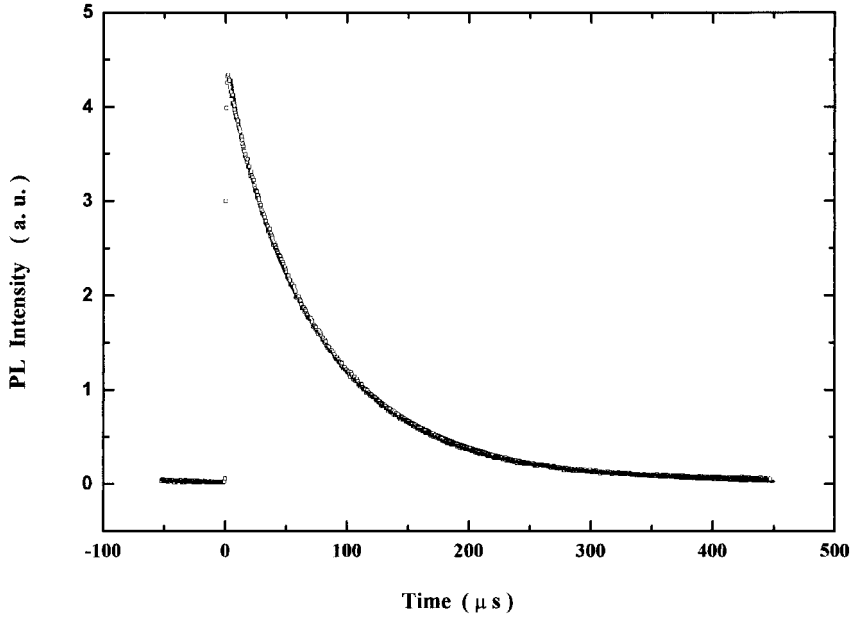

Figure 9. Simulation of the luminescence decay by energy transfer for the dipole–dipole type interaction ($N_{Nd} = 5.413 \times 10^{20}$ cm^{-3}) and the parameters: $\tau = 178$ μs and $R_0 = 8.4$ Å. (□): experimental; (· · · · · ·): theoretical.

transfer rates. The values of τ and R_0 obtained from this simulation are respectively almost equal to 178 μs and 8.4 Å. The latter parameter is larger than the mean distance ($R \sim 7.3$ Å) between Nd^{3+} ions ($R = (3/4\pi N)^{1/3}$) which means that energy transfer is very possible for concentration higher than 4.3×10^{20} cm^{-3}.

6. Conclusion

We have studied the spectroscopic properties of the Nd^{3+}-doped phosphate glasses. On the basis of the J–O theory, we have concluded that these materials have an intermediate cross-section and a weak Ω_4/Ω_6 parameter which indicates that the $^4F_{3/2} \rightarrow {}^4I_{11/2}$ laser emission is relatively intense. The evolution of this transition with respect to the concentration shows an intensity decrease for the concentration exceeding 4.3×10^{20} cm^{-3}. This phenomenon is attributed to cross-relaxation of these ions. Furthermore, an important thermal extinction was also observed between 9 and 100 K and associated to non-radiative relaxation due to the high vibration frequency of phosphate groups and to energy transfer to the OH^- ones which come from the persistent water in the initial composition.

References

[1] Marion J E and Weber M J 1991 *Eur. J. Solid State Inorg. Chem.* **28** 271
[2] Glas P, Naumann M, Schumarcher A, Müller H R, Reichel V and Unger S 1997 *Fiber Integrated Opt.* **16** 103
[3] Dawar A L, Mehta V, Mansingh A and Rup R 1997 *Opt. Mater.* **7** 33
[4] Adam J L, Sinektals F and Lucas J 1994 *Opt. Mater.* **4** 85
[5] Danilchuk N, Savostyanov V and Shapovalov V 1988 *Opt. Spectrosc.* **65** 538
[6] Judd B R 1962 *Phys. Rev.* **127** 750

[7] Ofelt S G 1962 *J. Chem. Phys.* **37** 511
[8] Shinn M D, Sibley W, Drexhage M G and Brown R N 1983 *Phys. Rev.* B **22** 6635
[9] Reisfeld R, Kisilev A, Buch A and Ish-Shalom M 1987 *J. Non-Cryst. Solids* **47** 33
[10] Krupke W F 1974 *IEEE J. Quantum Electron.* **10** 45
[11] Jørgensen C K and Reisfeld R 1983 *J. Less-Common Met.* **93** 107
[12] Auzel F 1979 *Mater. Res. Bull.* **14** 223
[13] Jacobs R R and Weber M J 1976 *IEEE J. Quantum Electron* **12** 102
[14] Tesar A, Campbell J, Weber M J, Weinzapfel C, Lin Y, Meissner H and Toratani H 1992 *Opt. Mater.* **1** 217
[15] Fuxi G 1992 *Optical and Spectroscopic Properties of Glass* (Berlin: Springer)
[16] Orazion S 1989 *Principles of Lasers* (New York: Plenum)
[17] Weber M J, Ziegler D C and Angell C A 1982 *J. Appl. Phys.* **53** 4344
Brecher B, Riseberg L A and Weber M J 1978 *Phys. Rev.* B **18** 5799
[18] Seeber W, Ehrt D and Ebendorff-Heidrpriem H 1994 *J. Non-Cryst. Solids* **171** 94
[19] Reisfeld R 1975 *Struct. Bonding* **22** 123
Ebendorff-Heidrpriem H, Seeber S and Ehrt D 1993 *Glastech. Ber.* **66** 235
[20] Toratani H, Izumitani T and Kuroda H 1982 *J. Non-Cryst. Solids* **52** 303
[21] Haouari M, Ben Ouada H, Maâref H, Hommel H and Legrand A P 1997 *J. Phys.: Condens. Matter* **9** 6711
[22] Miyakawa T and Dexter D L 1970 *Phys. Rev.* B **1** 2961
[23] Holstein T, Lyo S K and Orbach M 1981 *Laser Spectroscopy of Solids (Topics in Applied Physics 49)* ed W M Yen and P M Salzer (Berlin: Springer)
[24] Macho E, Balda R, Elejalde M J, Fernandez J and Adam J L 1993 *J. Non-Cryst. Solids* **161** 245
[25] Ebendorff-Heidrpriem H, Seeber W and Ehrt D 1993 *J. Non-Cryst. Solids* **163** 74
[26] Dexter D L 1953 *J. Chem. Phys.* **21** 836
[27] Inokuti M and Hyrayama F 1965 *J. Chem. Phys.* **43** 1978